Submitted: 15 February, 2023 Accepted: 25 April, 2023 Published: 30 May, 2023 DOI:10.22514/jomh.2023.039

ORIGINAL RESEARCH

JOMH Journal of Men's Health

Correlation of pain with substance P and neurokinin-1 receptor in the L5–S2 spinal cord in rats with chronic nonbacterial prostatitis

Liya Hao[1], Junfeng Zhang[1], Xianguang Bai[1], Xichao Xia[1], Xinhua Zheng[1], Yuebin Yuan[2,*]

[1]Departmemt of Basic Medicine, Medical College of Pingdingshan University, 467000 Pingdingshan, Henan, China
[2]Department of General Practice, 989th Hospital of Joint Logistic Support Force, 467000 Pingdingshan, Henan, China

***Correspondence**
yuanyuebin989@163.com
(Yuebin Yuan)

Abstract

The incidence of prostate pain is 90%–95% in prostatitis. The symptoms are persistent, which is prone to relapse and difficult to be cured. It seriously affects the survival and quality of life of patients. This study analyzed the correlation between pain and substance P (SP) and neurokinin-1 receptors (NK-1R) in the L5–S2 spinal cord of chronic nonbacterial prostatitis (CNP) rats, which may give a new way to explore the pathogenesis and treatment of pain in prostatitis. We randomly divided the rats into control group, 45 d group, 60 d group, and 90 d group. After making a rat model with autoimmune method, the paw withdrawal threshold (PWT) was measured, the histomorphological changes in the prostate was observed by transmission electron microscopy and light microscopy. The expression of SP and NK-1R was measured by immunohistochemistry, and the concentrations of tumor necrosis factor-α (TNF-α), interleukin-1β (IL-1β), interleukin-2 (IL-2), and interleukin-10 (IL-10) were measured by enzyme linked immunosorbent assay (ELISA). Compared with the control group, the PWT was decreased by 34.21%, 41.90% and 64.79%, TNF-α was increased by 74.19%, 89.45% and 132.15%, IL-1β was increased by 148.88%, 181.95% and 250.74%, IL-2 was increased by 75.97%, 82.15% and 128.57% and IL-10 was increased by 31.04%, 63.28% and 212.99% in the 45 d group, 60 d group and 90 d group respectively. Microscope observation showed the structure of prostate tissue in control group was normal. However, the prostate tissue had obvious inflammatory response with the model extension. The expressions of SP and NK-1R in each model group were significantly higher than the control group. There was a significant correlation between pain and SP in L5–S2 spinal cord in CNP rats. These findings are indicative of a correlation between pain and the expression levels of SP and NK-1R in the L5–S2 spinal cord of CNP rats.

Keywords

Chronic nonbacterial prostatitis; Pain; Substance P; Neurokinin-1 receptor; Rat model

1. Introduction

Chronic prostatitis (CP) is a common disease of the urological and reproductive systems of adult men [1] and accounts for about one quarter of outpatients [2]. Chronic nonbacterial prostatitis (CNP) is the most common type and accounts for 90% of all CPs [3, 4]. About 50% of men are affected by CNP [5]. At present, the pathogenesis, pathophysiology, and the underlying mechanisms of CNP are not very clear [6]. The clinical symptoms of CNP are complicated, and pain is the most obvious manifestation; however, the diagnosis and treatment are still medical challenges. Some scholars believe that the pain is not necessarily caused by the prostatic lesions and may instead be related to the abnormal nerve conduction pathways and regulatory mechanisms that govern the prostate, which are likely due to secondary lesions of the L5–S2 spinal cord segment [7]. Some scholars believe that when the nerve is stimulated, SP is released in the central and peripheral end respectively, and plays a physiological role in combination with NK-1R. SP released from the central segment can directly or indirectly participate in the transmission of pain by promoting the release of glutamate [8]. In this study, an autoimmune method was used to establish a CNP rat model. The expression of Substance P (SP) and its neurokinin-1 receptor (NK-1R) in the spinal dorsal horn of the L5–S2 spinal cord at different time periods were evaluated to explore the possible mechanisms of pain. Thus, it opens up a new way to study the pathogenesis and treatment mechanism of CNP pain.

2. Methods

2.1 Experimental animals

In all, 70 healthy adult male Sprague-Dawley rats weighing 250–300 g were provided by Qinglongshan Animal Breeding Farm in Jiangning District, Nanjing City (certificate number: SCXK (Su) 2018-0001). The rats were collectively housed under a 12-h light/dark cycle at a temperature of 25 ± 1 °C and a relative humidity of 55 ± 5%. Adequate food and water were available *AD libitum*, and they were Specific pathogen Freed.

2.2 Model building and grouping

The rat CNP model was established according to the study of Zhang Yaqiang *et al.* [9]. Thirty male Sprague Dawley (SD) rats weighing 280–300 g were sacrificed by grabbing the head of the rats with one hand and the tail of the rats with the other, and pulling with both hands at the same time until their cervical spines were broken, and the lower abdomen skin was disinfected. The prostate tissue was stripped and fully washed with cold physiological saline and a physiological saline solution (containing 0.5% TritonX-100, American Sigma). The prostate tissue was then homogenized (with the lower part of the glass homogenizer in ice) and centrifuged at 3000 × g for 30 min at 4 °C; The centrifuged supernatant was extracted, and the biuret method was used to determine the protein concentration (Biuret kit, Nanjing Jiancheng Technology Co., Ltd.). The prostatitis solution was diluted to 40 g/L with 0.1 mol/L PBS (pH 7.4) to establish the CNP rat model.

Forty male SD rats weighing 250–280 g were randomly divided into four groups: one control group and three model groups (45 days (d), 60 d, and 90 d), with 10 rats in each group. On days 0 and 30, animals in each group were anesthetized with ether. The model groups were injected intraperitoneally with 0.5 mL of diazepam vaccine (Wuhan Institute of Biological Products), while intradermal injections of 1 mL Freund's Complete Adjuvant (American Sigma) at a ratio of 1:1 and a suspension of prostate protein extract. The control group was injected with the same volume of saline.

2.3 Detection of paw withdrawal threshold (PWT)

PWT was measured using the Chaplan method, as described previously [10]. All rats were placed in a translucent glass cage, and Von Frey filaments were used to stimulate the midfoot of the hind limbs. Slight bending of the filaments was used as a standard force to bend the fibers into an S shape for 6–8 s. The rats were stimulated the rats sequentially with fiber filaments weighing 2, 4, 6, 8, 10, 15, 26 g for 2 s at intervals of 15 s. This procedure was repeated 5 consecutive times. The minimum number of grams needed to induce leg lifts in three out of the five replicates was defined as PWT. PWT was measured at 45, 60 and 90 days, after modeling began.

2.4 Light microscopy, transmission electron microscopy, and SP and NK-1R immunohistochemistry

2.4.1 Take material

At 45, 60 and 90 days after modeling, the rats died due to cervical spine laceration. The prostate tissues of rats in each group were taken and observed under light and transmission electron microscope. The L5–S2 segments of the spinal cord were removed for SP and NK-1R immunohistochemistry.

2.4.2 Examination of light microscopy

Part of the prostate tissues were fixed with 4% neutral formaldehyde solution at room temperature for 24 hours, then dehydrated in ethanol gradient, transparent and soaked in xylene, embedded in paraffin, sectioned, 4 μm thick, and stained with hematoxylin-eosin (HE). The structural and morphological changes of the prostate tissue were observed under an optical microscope (Olympus Optical Co., LTD., Japan).

2.4.3 Transmission electron microscopic observation

The remaining prostate tissue was cut into 1 mm × 1 mm × 1 mm pieces, double fixed in 4.9% glutaraldehyde and 1% osmic acid (PH = 7.4), dehydrated in ethanol and acetone, embedded in Epon 812 epoxy resin and sectioned. Ultrathin sections were stained with uranyl acetate and lead citrate. The microstructures of the prostate tissue were observed under a H-7500 transmission electron microscope (Hitachi, Japan).

2.4.4 SP and NK-1R immunohistochemistry

The spinal cord was removed and fixed in 4% paraformaldehyde phosphate buffer and kept in the refrigerator 4 °C overnight. The L5–S2 spinal cord segment was isolated, and continuous cross-sections were obtained using a vibrating microtome, and floating immunohistochemistry on freely floating fixed tissue sections (American Sigma) was performed to detect the optical density (OD) values of SP and NK-1R immunopositive reactions.

2.5 Determination of tumor necrosis factor-α (TNF-α), interleukin-1β (IL-1β), interleukin-2 (IL-2) and interleukin-10 (IL-10) in prostate tissues

Briefly, 1 mL of 0.5% TritonX-100 normal saline per 100 mg of prostate tissue was added to prepare the tissue homogenate, and centrifuged at 3000 × g for 15 min. The concentrations of TNF-α, IL-1β, IL-2 and IL-10 in the prostate tissues was measured in an appropriate amount of supernatant by using ELISA method (American Sigma).

2.6 Statistical analysis

Descriptive and differential statistical analysis of the data were conducted. For normal distribution, the mean and standard deviation were used to describe the centralized and discrete trends, respectively. The variances were the same. A completely random design analysis of variance was used, and the Student-Newman-Keuls-q (SNK-q)method was used to compare pairs. And the correlation analysis was done. The test standard was $\alpha = 0.05$. The SAS 9.1 software (North Carolina

State University, Cary, NC, United States) was used for all statistical analysis.

3. Results

3.1 PWT changes

Compared with the control group, the PWT of rats in the 45 d, 60 d and 90 d groups decreased. The PWT in the 90 d group was significantly lower than that in the 45 d and 60 d (all $p < 0.05$) groups (Table 1). The pain sensitivity of rats appeared to be enhanced after modeling, and the pain was more sensitive with increasing modeling time.

3.2 Pathological examination of prostate tissue under light microscopy

The prostate tissue of the control group appeared normal (Fig. 1A). Lymphocyte infiltration around the capillaries and irregular glandular cavity were visible in the prostate tissue in the CNP rat model at 45 days after modeling (Fig. 1B). Interstitial edema, large numbers of lymphocyte infiltration around the capillaries, and invasion of the local glandular epithelium into the prostate cavity were more obvious in the CNP model, with part of the basement membrane widened or destroyed and intraluminal secretions increased or decreased, at 60 days after modeling (Fig. 1C). A large number of lymphocytes and mast cells were found in the CNP model, with a few neutrophils and plasma cells where the epithelium appeared segmental necrosis and shedding. The glandular cavity was dilated, no secretions were seen in part of the prostate cavity, and interstitial collagen fibers showed proliferation at 90 days (Fig. 1D).

3.3 TEM pathological results of prostate tissue

The structure of the prostate was normal in the control group, with a small number of mitochondria, rich rough endoplasmic reticulum, developed Golgi complex, and a large amount of secretions in the glandular cavity (Fig. 2A). At 45 days after modeling, epithelial cells proliferated and the interstitial space widened, endoplasmic reticulum was abundant, and mast cells were visible in the interstitial space (Fig. 2B). Infiltration of macrophages and lymphocytes was seen around capillaries at 60 days after modeling, with widened epithelial space of the prostate and exacerbated peritubular and interstitial edema (Fig. 2C). Interstitial edema was more pronounced, with the space between the peritubular cells and the base of the epithelium was widened, and the number of fibroblasts and surrounding collagen fibrils increased at 90 days after modeling (Fig. 2D).

3.4 Comparison of TNF-α, IL-1β, IL-2 and IL-10 concentrations in prostate tissue of rats in each group

Compared with the control group, the concentrations of TNF-α, IL-1β, IL-2 and IL-10 in the prostate tissue of each model group was significantly increased. However, this increase was most significant in the 90 d group (all $p < 0.05$) (Table 2). Inflammation was seen in the prostate tissue of rats after modeling, and the inflammation became more severe as the modeling time increased.

3.5 Immunohistochemical results of SP and NK-1R in the L5--S2 spinal cord of rats in each group

Light microscopy showed that both SP and NK-1R immunoreactants were densely packed in the dorsal horn of the spinal cord, which was distributed in a brown-yellow cord-like form, while other parts were either not colored or pale yellow (Figs. 3,4). The OD value of each model group was significantly higher than that of the control group, while the OD value of the 90 d group was higher than that of the remaining three groups (Tables 3,4) (all $p < 0.05$), which suggested that SP synthesis in the L5–S2 spinal dorsal horn in CNP rats increased, causing the receptor to be up-regulated. This was more significant with increasing modeling time.

3.6 Correlation between pain and SP at different spinal segments in CNP rats

There was a significant correlation between pain and SP in L5–S2 spinal cord in CNP rats (Table 5) ($r = -0.957$, $r = -0.962$, $r = -0.943$, $r = -0.949$; all $p < 0.05$).

4. Discussion

The disease course of CNP is long and presents with complex symptoms [11], which seriously affect patients' quality of life and physical and mental health [12–14]. According to global statistics, the incidence of CNP ranges from 2.2% to 9.7%, with an average prevalence of 8.2% [15]. The pathogenesis and pathophysiology of CNP are not very clear, and the treatment is challenging [16]. Persistent and intractable pain that is difficult to control with drugs is a characteristic feature of CNP. It is also the most important symptom that affects the quality of life of patients and the main reason for outpatient visits [17], while CNP is as severe as active Crohn's disease, myocardial infarction, and unstable angina [18].

CNP pain sensitivity is increasing, which is mostly chronic, persistent, spontaneous, recurrent and intractable in the pelvis Some scholars believe that inflammation is only one of the causes of prostate pain [19], whereas others suggested that while CNP pain may be due to a single cause, there were many factors that contributed to the gradual development of a chronic neuropathic state as the disease progressed [20]. This pain may be related to secondary lesions of the L5–S2 spinal segment that dominated the prostate [21]. After Chen *et al.* [21] chemically stimulated the bladder, prostate, and involved pain sites (root of tail) in rats, the expression of c-fos-positive cells in the lumbosacral spinal cord was abundant, while the distribution of c-fos-positive cells was similar in these three areas [21]. Zhang *et al.* [22]'s study showed that highly expressed SP was involved in the generation and maintenance of neuropathic pain. Xu *et al.* [23] found that plasma SP levels in patients with CNP were significantly higher than those in the control group, suggesting that the expression of SP was closely related to the occurrence and development of CNP. Through

TABLE 1. Paw withdrawal threshold (PWT) of the rats in the control and different modeling groups ($\bar{x} \pm s$).

Group	n	PWT (g)
Control	10	73.34 ± 6.86
Model		
45 d	10	48.25 ± 6.65^{a}
60 d	10	42.61 ± 4.93^{ab}
90 d	10	25.82 ± 5.73^{abc}

a: $p < 0.05$ vs. the control group; b: $p < 0.05$ vs. the 45 d group; c: $p < 0.05$ vs. the 60 d group.

TABLE 2. Levels of TNF-α, IL-1β, IL-2 and IL-10 in the prostate tissue of rats in the control and different modeling groups ($\bar{x} \pm s$).

Group	n	TNF-α (pg/mL)	IL-1β (pg/mL)	IL-2 (pg/mL)	IL-10 (pg/mL)
Control	10	41.34 ± 2.21	15.57 ± 1.02	68.86 ± 7.21	90.09 ± 16.85
Model					
45 d	10	72.01 ± 2.23^{a}	38.75 ± 3.74^{a}	121.17 ± 9.49^{a}	118.05 ± 12.53^{a}
60 d	10	78.32 ± 3.23^{ab}	43.90 ± 2.44^{ab}	125.43 ± 10.12^{ab}	147.10 ± 8.91^{ab}
90 d	10	95.97 ± 7.06^{abc}	54.61 ± 1.92^{abc}	157.39 ± 9.52^{abc}	281.97 ± 9.31^{abc}

a: $p < 0.05$ vs. the control group; b: $p < 0.05$ vs. the 45 d group; c: $p < 0.05$ vs. the 60 d group.

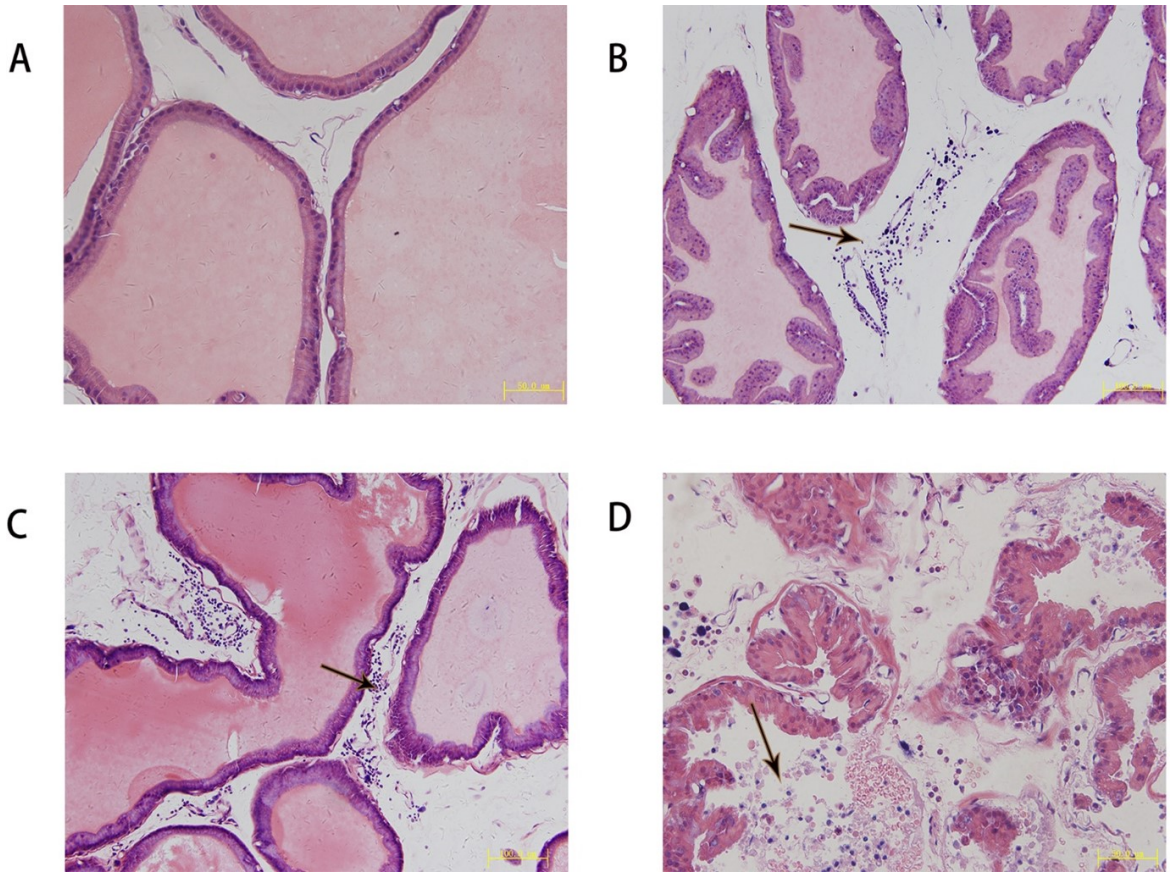

FIGURE 1. Results of HE staining of the prostate tissue from different groups of rats (scale bar: 50 μm). (A) No inflammatory cells infiltration was seen in the prostate tissue of the control rats. (B) Lymphocytes were visible in the prostate tissue from the rat model of chronic nonbacterial prostatitis (CNP) at 45 days after modeling. (C) Edema was more obvious in the CNP rat model, with large numbers of lymphocytes at 60 days after modeling. (D) A large number of lymphocytes and mast cells were found in the CNP rat model, with a few neutrophils and plasma cells at 90 days. The black arrows indicate lymphocytes. The glandular cavity was expanded and collagen fibers were proliferated. Bar = 50 μm.

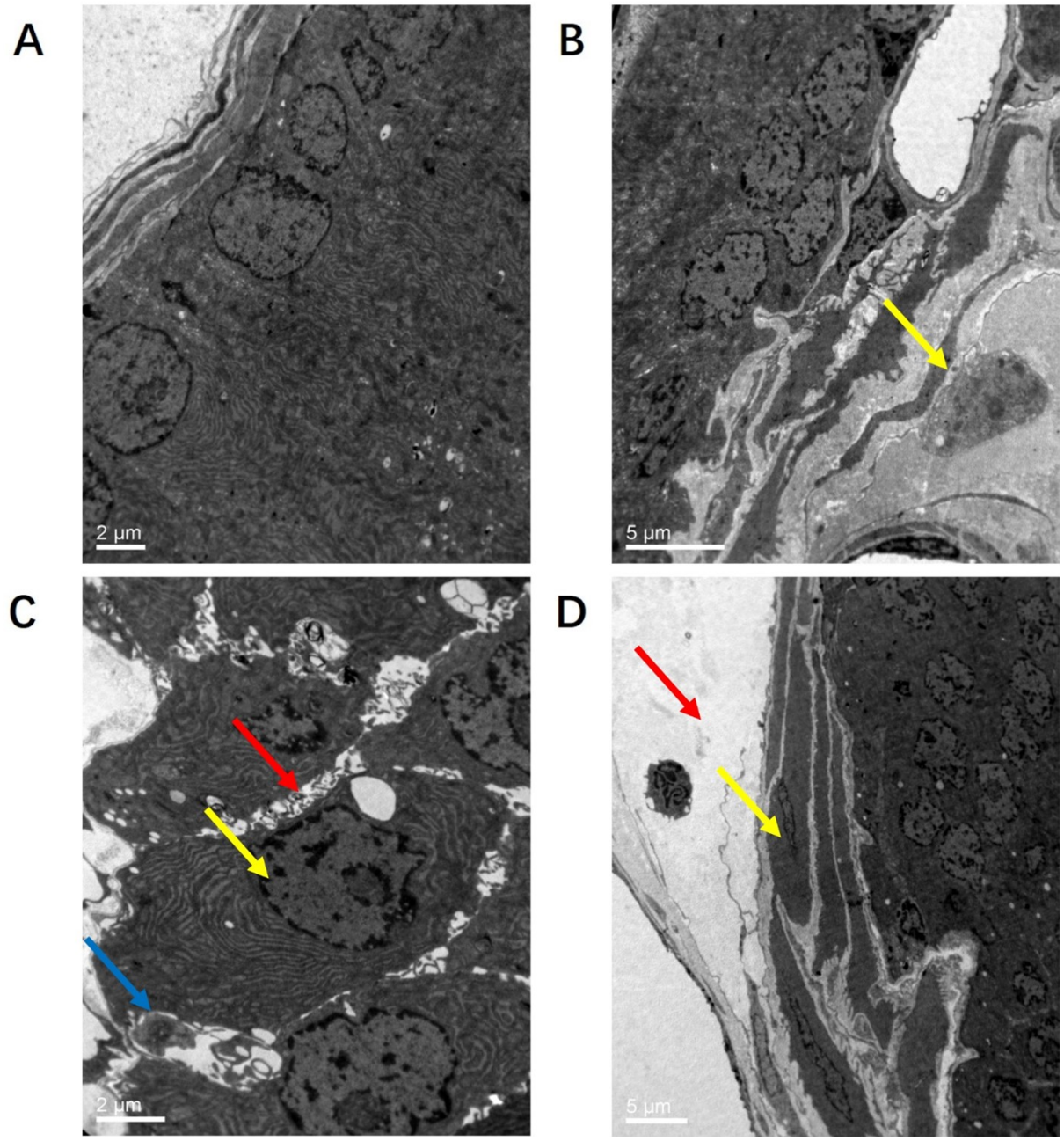

FIGURE 2. Prostate tissues from different groups of rats as observed under transmission electron microscopy. (A) The structure of the prostate was normal in the control group. (B) Mast cells were observed at 45 days after modeling. The yellow arrow indicates mast cells. (C) Widened intercellular space (the red arrow) of the epithelium along with lymphocytes (the blue arrow) and macrophages (the yellow arrow) were seen at 60 days after modeling. (D) Fibrosis (the yellow arrow) and edema (the red arrow) were found in the Prostate interstitial at 90 days after modeling.

TABLE 3. Optical density of Substance P (SP) in the posterior horn of the L5–S2 spinal cord in different groups of rats ($\bar{x} \pm s$).

Group	n	L5	L6	S1	S2
Control	10	0.10 ± 0.02	0.10 ± 0.02	0.09 ± 0.01	0.09 ± 0.01
Model					
45 d	10	0.17 ± 0.03^{a}	0.17 ± 0.03^{a}	0.14 ± 0.01^{a}	0.15 ± 0.02^{a}
60 d	10	0.19 ± 0.02^{ab}	0.21 ± 0.06^{ab}	0.18 ± 0.04^{ab}	0.18 ± 0.03^{ab}
90 d	10	0.28 ± 0.03^{abc}	0.27 ± 0.03^{abc}	0.26 ± 0.03^{abc}	0.26 ± 0.03^{abc}

a: $p < 0.05$ vs. the control group; b: $p < 0.05$ vs. the 45 d group; c: $p < 0.05$ vs. the 60 d group.

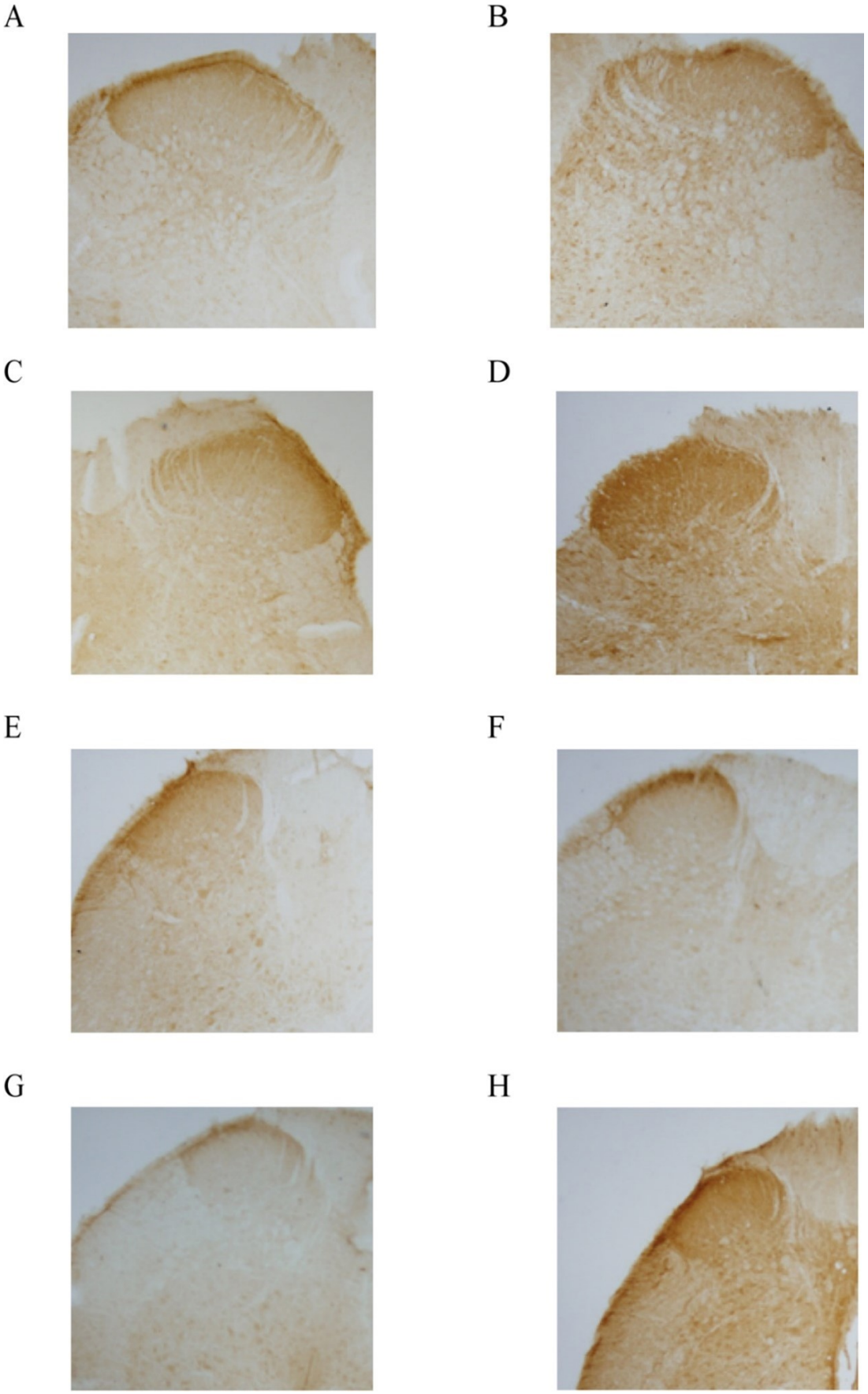

FIGURE 3. Expression of Substance P (SP) in the posterior horn of the L5–S2 spinal cord in different groups of rats (IHC: 40×). (A) L5 in the control group; (B) L5 in the 60 d modeling group; (C) L6 in the control group; (D) L6 in the 60 d modeling group; (E) S1 in the 60 d modeling group; (F) S1 in the 90 d modeling group; (G) S2 in the control group; (H) S2 in the 90 d modeling group.

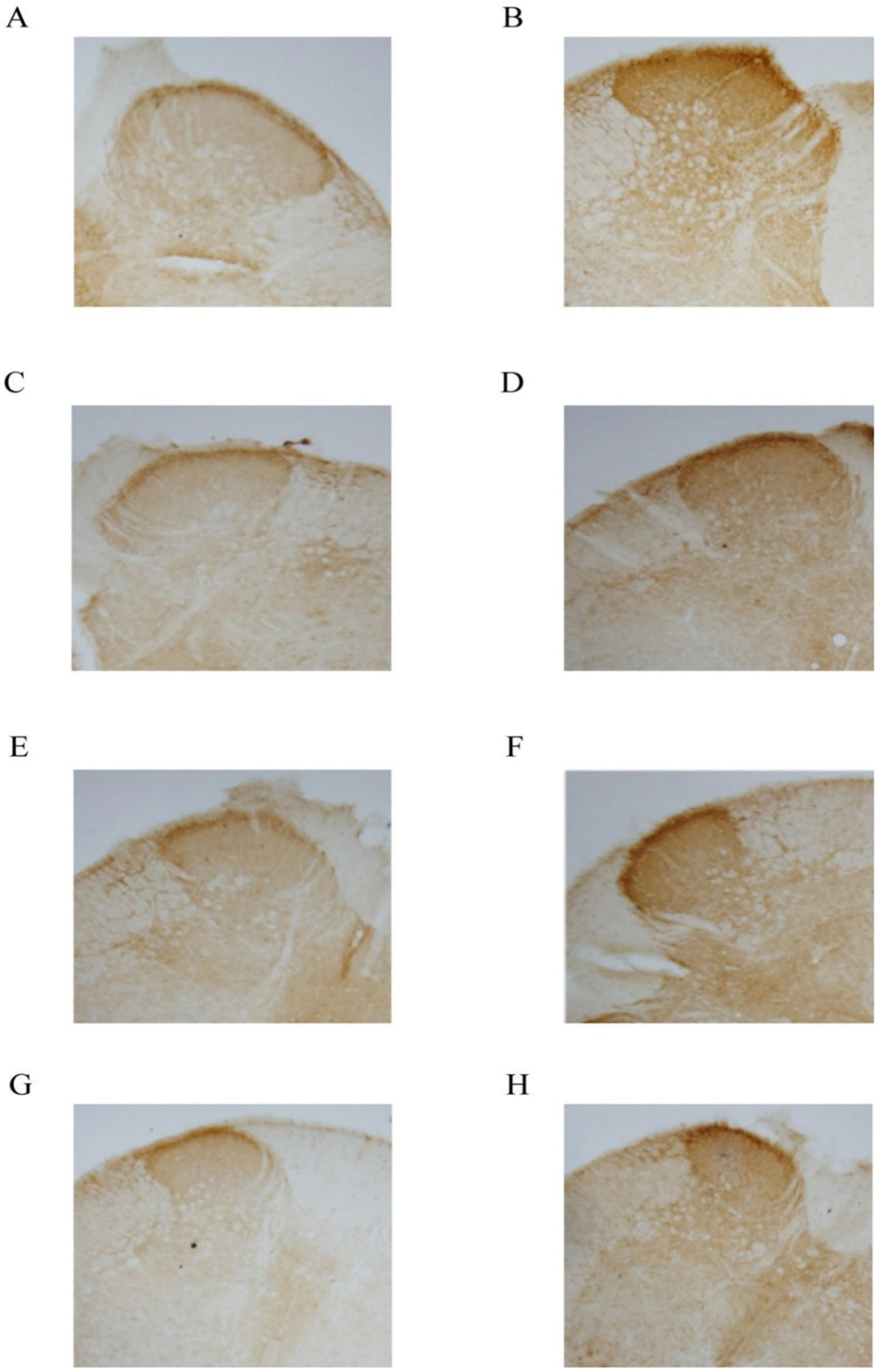

FIGURE 4. Expression of neurokinin-1 receptor (NK-1R) in the posterior horn of the L5–S2 spinal cord in different groups of rats (IHC: 40×). (A) L5 in the control group; (B) L5 in the 90 d modeling group; (C) L6 in the control group; (D) L6 in the 45 d modeling group. (E) S1 in the control group; (F) S1 in the 90 d modeling group; (G) S2 in the control group; (H) S2 in the 60 d modeling group.

TABLE 4. Optical density of neurokinin-1 receptor (NK-1R) in the posterior horn of the L5–S2 spinal cord in different groups of rats ($\bar{x} \pm s$).

Group	n	L5	L6	S1	S2
Control	10	0.08 ± 0.01	0.08 ± 0.01	0.07 ± 0.01	0.07 ± 0.01
Model					
45 d	10	0.15 ± 0.01^{a}	0.16 ± 0.01^{a}	0.14 ± 0.01^{a}	0.14 ± 0.01^{a}
60 d	10	0.19 ± 0.01^{ab}	0.19 ± 0.01^{ab}	0.18 ± 0.04^{ab}	0.18 ± 0.01^{ab}
90 d	10	0.26 ± 0.01^{abc}	0.26 ± 0.01^{abc}	0.25 ± 0.01^{abc}	0.24 ± 0.01^{abc}

a: $p< 0.05$ vs. the control group; b: $p< 0.05$ vs. the 45 d group; c: $p< 0.05$ vs. the 60 d group.

TABLE 5. Correlation between pain and SP in the L5–S2 spinal cord in CNP rats.

OD	PWT (n = 40)	n	r	*p*
L5		40	−0.957	0.000
L6		40	−0.962	0.000
S1		40	−0.943	0.000
S2		40	−0.949	0.000

OD: optical density; PWT: paw withdrawal threshold.

further analysis, they found that plasma SP levels gradually increased with the progression of the disease which suggested a certain relationship between the SP levels and degree of the patient's condition [23].

SP is an important pain transmitter. When noxious stimuli appear, SP is transmitted to the central nervous system. At the same time, the reverse release of SP was also found in the damaged local tissues, which can cause neurogenic inflammatory reactions that are closely related to the occurrence of inflammatory pain, hyperalgesia, and neurogenic pain and are involved in the transmission of peripheral pain stimuli to the center [24]. SP mainly exists on the C fibers of the spinal cord and is released in the spinal dorsal horn, where SP receptors are rich, and activates NK-1R to transmit pain information. Some scholars believe that the combination of SP and NK-1R mediates the production of pain [25]. When the nerve is stimulated, SP is released at the central and peripheral ends and combines with NK-1R to exert a physiological role. After being released from the central segment, SP can directly or indirectly participate in pain transmission by promoting the release of glutamic acid and aspartic acid [8]. Through *in vivo* experiments, some researchers have found the lowest limit of L- and T-type calcium channel blockers affecting the release of SP from rats injected with formalin, by detecting the internal changes of neurokinin receptors [26].

Studies have shown that the pathological changes of CP/CPPS animal model established by autoimmune reaction are most similar to those of clinical practice, and the pathogenesis is also more consistent with [9]. Moreover, it does not cause pathological changes in other organs, and only leads to autoimmune response in prostate tissue, which has good specificity and is an ideal modeling method [27]. In this study, different degrees of chronic inflammation and proliferative pathological changes were observed in the prostate of rats in different groups. While the levels of TNF-α, IL-1β, IL-2 and IL-10 increased, the PWT in rats decreased, which suggested an increased sensitivity to pain, thereby indicating that the CNP model established by the autoimmune method was successful. The expressions of SP and NK-1R in the dorsal horn of L5–S2 spinal cord in the 45 d, 60 d and 90 d groups were higher than those in the control group, the difference was statistically significant ($p < 0.05$); this result was consistent with the findings of Xu [23] and Liu [28]. SP can also stimulate the secretion of cytokines such as TNF-α and IL-1β, which further aggravate chronic inflammation of the prostate and cause increased pain. The PWT of the 45 d, 60 d and 90 d groups was lower than the PWT of the control group. The PWT of the 90 d group was lower than those of the 45 d and 60 d group ($p < 0.05$), further proving that SP can aggravate the degree of pain in CNP models. Correlation analysis was performed between the PWT and the OD value of SP in the L5, L6, S1, S2 spinal cord of all groups of rats, and the results showed r = −0.957, r = −0.962, r = −0.943, r = −0.949 (all $p < 0.05$). This proved that there was a significant correlation between pain and SP in L5–S2 spinal cord in CNP rats.

The pain manifestations of CNP are complex, often characterized by chronic attacks, persistent pain, variable pain sites, and difficulty in curing [29]. The complexity of CNP pain originates from the diversity of pain causes and the complexity of pathogenesis. Some scholars believe that this pain is not necessarily caused by the disease of the prostate itself, but may be related to the abnormal nerve conduction pathways and regulatory mechanisms that innervate the prostate, which may be caused by the secondary lesions of the L5–S2 spinal cord segment [30]. SP is mainly found in the C-fibers of the spinal cord and is released into the dorsal horn of the spinal cord, which is rich in SP receptors and activates NK-1R to transmit pain information. Some scholars believe that the combination of SP and NK-1R mediates the production of pain sensation [25]. When the nerve is stimulated, SP is released in the central and peripheral end, respectively, and plays a physiological role

by combining with NK-1R. SP released in the central segment can directly or indirectly participate in the transmission of pain by promoting the release of glutamate [8].

CNP is a slow and chronic disease with very complex and pathological processes. In this rat model of CNP, we extended the disease duration to 45, 60 and 90 days to investigate the expression of SP and NK-1R in the posterior horn of the L5–S2 spinal cord at the different time points of modeling. The results were significantly different for the studied time points, suggesting that the expressions of SP and NK-1R are a dynamic process, which is more in line with clinical manifestations.

In this study, the rat CNP model was prepared by the method of immune adjuvant, and the morphological changes of prostate tissue were observed at different time points. The pathological results were very similar to clinical results, which had more clinical significance. At the same time, the differential expression of SP and its receptor in the lumbosacral segment of the spinal cord was studied in rats under CNP, in order to provide experimental data for clinical selection of drugs targeting SP receptors for the treatment of CNP. However, this study has some limitations, and the specific mechanism of CNP pain needs to be further studied in depth.

5. Conclusions

In summary, the expression of SP and NK-1R in the spinal dorsal horn of L5–S2 of CNP rats is up-regulated, and the changes are different at different time periods, which is closely related to the refractory pain of chronic prostatitis. The conclusion of this study suggests that clinical research on new drugs that adjust nerves or adjust inflammatory cytokines to relieve pain from chronic prostatitis, the specific mechanism of which needs to be further studied.

ABBREVIATIONS

SP: substance P; NK-1R: neurokinin-1 receptor; CNP: chronic nonbacterial prostatitis; PWT: paw withdrawal threshold; CP: chronic prostatitis.

AVAILABILITY OF DATA AND MATERIALS

The data are contained within this article.

AUTHOR CONTRIBUTIONS

LYH, XHZ and YBY—designed the study and carried them out, prepared the manuscript for publication and reviewed the draft of the manuscript; LYH, JFZ, XGB and XCX—supervised the data collection, analyzed the data, interpreted the data. All authors have read and approved the manuscript.

ETHICS APPROVAL AND CONSENT TO PARTICIPATE

Ethical approval was obtained from the experimental animal ethics requirements of Shanghai University of Traditional Chinese Medicine (ethics approval number: SZY201807016). Written informed consent was obtained from a legally authorized representative(s) for anonymized patient information to be published in this article.

ACKNOWLEDGMENT

Not applicable.

FUNDING

This research was supported by Henan Province Colleges and Universities Science and Technology Research Key Project, 2021 (No.21B310005). 21B310005 is mainly used for the purchase of reagents and instruments.

CONFLICT OF INTEREST

The authors declare no conflict of interest.

REFERENCES

[1] Shang Y, Liu C, Cui D, Han G, Yi S. The effect of chronic bacterial prostatitis on semen quality in adult men: a meta-analysis of case-control studies. Scientific Reports. 2014; 4: 7233.

[2] Kulchavenya EVK, Shvetsova OPS, Breusov AAB. Rationale of use and effectiveness of Longidaza in patients with chronic prostatitis. Urologiia. 2018; 64–71. (In Russian)

[3] Han P, Lai YJ, Chen J, Zhang XN, Chen JL, Yang X. Protective potential of the methanol extract of Macrothelypteris oligophlebia rhizomes for chronic non-bacterial prostatitis in rats. Pakistan Journal of Pharmaceutical Sciences. 2016; 29: 1217–1222.

[4] Chen YZ, Gong XY, Zheng W, Xue CH, Li YQ. Interventional mechanism of Qianlie Huazhuo pill in rats with chronic nonbacterial prostatitis. Journal of Anhui University of Chinese Medicine. 2018; 37: 4. (In Chinese)

[5] Hajighorbani M, Ahmadi-hamedani M, Shahab E, Hayati F, Kafshdoozan K, Keramati K, *et al*. Evaluation of the protective effect of pentoxifylline on carrageenan-induced chronic non-bacterial prostatitis in rats. Inflammopharmacology. 2017; 25: 343–350.

[6] Huang M, Huang Q, Wu J, Qin T, Meng D, Urology DO. Correlation between the regulation of TGF-β1 signaling pathway by miR-150 and chronic nonbacterial prostatitis. Journal of Youjiang Medical University for Nationalities. 2019; 41: 489–499, 504.

[7] Middeldorp J, Hol EM. GFAP in health and disease. Progress in Neurobiology. 2011; 93: 421–443.

[8] Lagerström MC, Rogoz K, Abrahamsen B, Lind A, Ölund C, Smith C, *et al*. A sensory subpopulation depends on vesicular glutamate transporter 2 for mechanical pain, and together with substance P, inflammatory pain. Proceedings of the National Academy of Sciences. 2011; 108: 5789–5794.

[9] Zhang YQ, Wang Y, Li M, Lu XJ, Gao YS, Liu B, *et al*. Establishment of a rat model of autoimmune prostatitis induced by prostate tissue antigen protein. Chinese Journal of Integrated Traditional and Western Medicine Surgery. 2008; 14: 584–587.

[10] Chaplan SR, Bach FW, Pogrel JW, Chung JM, Yaksh TL. Quantitative assessment of tactile allodynia in the rat paw. Journal of Neuroscience Methods. 1994; 53: 55–63.

[11] Gao W, Li Q, Liu YQ, Li HS, Shi CX. Clinical study on treating chronic pelvic pain syndrome with moxibustion. Primary Medical Forum. 2020; 24: 3.

[12] Xu X, Hou J, Lv J, Huang Y, Pu J, Wang L. Overexpression of lncRNA GAS5 suppresses prostatic epithelial cell proliferation by regulating COX-2 in chronic non-bacterial prostatitis. Cell Cycle. 2019; 18: 923–931.

[13] Magri V, Marras E, Restelli A, Wagenlehner FME, Perletti G. Multimodal therapy for category III chronic prostatitis/chronic pelvic pain syndrome in UPOINTS phenotyped patients. Experimental and Therapeutic Medicine. 2015; 9: 658–666.

[14] Magistro G, Wagenlehner FME, Grabe M, Weidner W, Stief CG, Nickel JC. Contemporary management of chronic prostatitis/chronic pelvic pain syndrome. European Urology. 2016; 69: 286–297.

[15] Guu S, Geng J, Chao I, Lin H, Lee Y, Juan Y, *et al*. Efficacy of low-intensity extracorporeal shock wave therapy on men with chronic pelvic pain syndrome refractory to 3-as therapy. American Journal of Men's Health. 2018; 12: 441–452.

[16] Wang HZ, Li M. Treating 50 cases of chronic prostatitis with Qingreishitongyu decoction. Chinese Medicine Science and Technology. 2019; 26: 2. (In Chinese)

[17] Nickel JC, Nyberg LM, Hennenfent M. Research guidelines for chronic prostatitis: consensus report from the first national institutes of health international prostatitis collaborative network. Urology. 1999; 54: 229–233.

[18] Krieger J, Ross S, Riley D. Chronic prostatitis: epidemiology and role of infection. Urology. 2002; 60: 8–12.

[19] Fogg RN, Mydlo JH. Nonbacterial infections of the genitourinary tract. Practical Urology: Essential Principles and Practice. 2011; 30: 323–337.

[20] Schaeffer AJ. Etiology and management of chronic pelvic pain syndrome in men. Urology. 2004; 63: 75-84.

[21] Chen Y, Song B, Jin X, Xiong E, Zhang J. Possible mechanism of referred pain in the perineum and pelvis associated with the prostate in rats. Journal of Urology. 2005; 174: 2405–2408.

[22] Zhang JH, Han LW, Qu JB, Zhou HC, Jia YR, Liu JF. Effect of pregabalin on expression of GFAP and SP in spinal cord of CCI model rats. Chinese Journal of Pain Medicine. 2018; 24: 6.

[23] Peng XU, Sikandaer, Wang Y, Center U. Correlation analysis of the expression of SP and β-endorphin with chronic pelvic pain syndrome. Chinese Journal of Human Sexuality. 2018; 27: 91–94. (In Chinese)

[24] Howard F. Chronic pelvic pain. Obstetrics & Gynecology. 2003; 101: 594–611.

[25] Muñoz M, Coveñas R. Involvement of substance P and the NK-1 receptor in human pathology. Amino Acids. 2014; 46: 1727–1750.

[26] Takasusuki T, Yaksh TL. Regulation of spinal substance P release by intrathecal calcium channel blockade. Anesthesiology. 2011; 115: 153–164.

[27] Wen ZP, Hong ZM, Lin XY, Lin F, Quan L, Wang Y, *et al*. Effect of Qianlie Huoxue decoction on inflammatory factors in the prostate of rats with autoimmune prostatitis. World Journal of Integrated Chinese and Western Medicine. 2010; 5: 396–400. (In Chinese)

[28] Liu Y, Song G, Zhang C. Prostatic inflammation-induced chronic pelvic pain: roles of substance P and c-fos in the spinal cord. National Journal of Andrology. 2015; 21: 681–686.

[29] Du H, Zhao WM. The pathogenesis of pain in chronic prostatitis. Journal of Modern Urology. 2017; 22: 76–78.

[30] Middeldorp J, Hol EM. GFAP in health and desease. Progress in Neurobiology. 2011; 93: 421–443.

How to cite this article: Liya Hao, Junfeng Zhang, Xianguang Bai, Xichao Xia, Xinhua Zheng, Yuebin Yuan. Correlation of pain with substance P and neurokinin-1 receptor in the L5–S2 spinal cord in rats with chronic nonbacterial prostatitis. Journal of Men's Health. 2023; 19(5): 36-45. doi: 10.22514/jomh.2023.039.